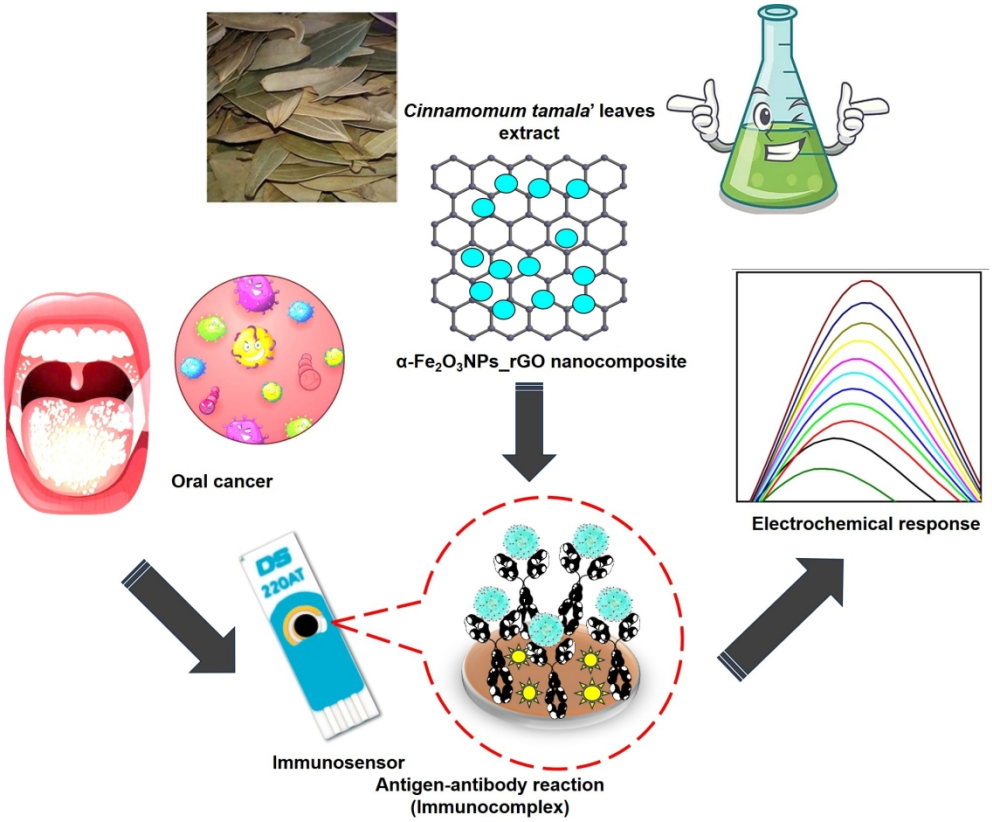

343x283mm (150 x 150 DPI)

IEEE Sensors Letters
Chemical and biological sensor

An Ultrasensitive Electrochemical Immunosensor Comprising Green Synthesized α-Fe_2O_3NPs_rGO Nanocomposite for Determination of Oral Cancer

Damini Verma[1], Sumit K Yadav[2], Ashish Kalkal[3], Rangadhar Pradhan[2]*, Gopinath Packirisamy[1,4]*

[1] *Centre for Nanotechnology, Indian Institute of Technology Roorkee, Roorkee, Uttarakhand, 247667, India*
[2]*iHub Divyasmapark, Technology Innovation Hub, Indian Institute of Technology Roorkee, Roorkee, Uttarakhand, India-247667*
[3]*Nanostructured system Laboratory, Department of Mechanical Engineering, University College London, London, WC1E 7JE UK*
[4] *Department of Biosciences and Bioengineering, Indian Institute of Technology Roorkee, Roorkee, Uttarakhand, 247667, India*

Abstract— Oral squamous cell carcinoma (OSCC) is a commonly known malignant tumor in the maxillofacial and oral region with a poor prognosis. Therefore, in the present letter, we have developed for the first time screen printed electrode (SPE) based affordable, simple, and ultrasensitive electrochemical immunosensor using a green synthesized hematite nanoparticles (α-Fe_2O_3NPs) supported on reduced graphene oxide (rGO) nanocomposite for determination of CYFRA-21-1 cancer biomarker. The α-Fe_2O_3NPs_rGO composite has been prepared using a green method employing the leaves extract *of Cinnamomum tamala*. The 3-aminopropyl triethoxysilane (APTES) helped in functionalization of α-Fe_2O_3NPs_rGO nanocomposite and was drop-casted to the working area of SPE, followed by immobilization with the anti-CYFRA-21-1 antibodies as well as bovine serum albumin (BSA) to form BSA/anti-CYFRA-21-1/APTES/α-Fe_2O_3NPs_rGO/SPE immunoplatform. The α-Fe_2O_3NPs_rGO nanocomposite were characterized utilizing the fourier transform infrared spectroscopy (FTIR), X-ray diffraction (XRD), differential pulse voltammetry (DPV) as well as cyclic voltammetry (CV) for investigating the crystal structure, as well as electrochemical properties. The developed immunosensor depicted remarkable electrochemical properties having broad linearity (0.5-20 ng/mL), limit of quantification (LOQ) of 0.048 ng/mL, low detection limit of 0.014 ng/mL, and high sensitivity of 90.42 μA (log (ng/mL)$^{-1}$ cm^{-2}. In addition, it showed high reproducibility and good selectivity towards the CYFRA-21-1 biomarker. Thus, this letter unlocks innovative prospects for exploring the electrochemical behavior of green synthesized α-Fe_2O_3NPs_rGO and its efficacy for fabricating electrochemical biosensors as well as point of care (POC) sensing devices.

Index Terms— Oral cancer, Electrochemical detection**,** Nanocomposite, Immunosensor

I. INTRODUCTION

Oral squamous cell carcinoma also known as OSCC is one of the most prevalent form of oral cancer of cavity and is the major source of mortality rate in developing nations [1]. Though at early levels, the survival rate ranges from 80% to 90%, but it gets lower to only 15-50% in advanced stages [2]. Currently, various traditional techniques reported for monitoring and determination of oral cancer, such as biopsy, cytopathology, visualization adjuncts, enzyme linked immunosorbent assay (ELISA), and laser capture microdissection, but due to their invasive, expensive, complex, labor intensive, and time-consuming issues [3], there arises a critical requirement for suitable technique availability for early determination of oral cancer.

As initial OSCC monitoring is vital for the effective cancer treatment and long-term survival of cancer patients, clinical assessment utilizing cancer biomarkers is regarded as helpful for prognostic monitoring and early diagnosis with histopathological examination as per the molecular biology advancement. CYFRA-21-1 (cytokeratin 19 soluble fragment) is the most commonly found oral cancer biomarker, having a 40 kDa molecular weight. It is an acidic cytokeratin released from the cells as soluble fragments. The level of CYFRA-21-1 cancer biomarker is reported as 3.8 ng/mL in healthy individuals, while it rises to 17.46 ± 1.46 ng/mL in patients affected with oral cancer [4].

In recent years, biosensors have gained considerable attention and are affordable tools for detecting oral cancer. Amongst the different biosensors, electrochemical biosensors are regarded as quite promising as they are cost-effective, simple, specific, need low sample volume, as well as not affected by the turbidity of the sample [5]. Additionally, these devices can be miniaturized easily and converted into point-of-care (POC) devices [6]. The performance of electrochemical biosensor mainly depends on the nanomaterial's physiochemical properties comprising the immobilized biomolecules [7]. Therefore, biosensor surface modification with nanocomposite or nanomaterials is required to improve the electrode's sensitivity and oriented biomolecule immobilization.

Reduced graphene oxide (rGO), is a renowned potential sensing matrix owing to their semiconductor properties [8]. As the whole graphene oxide (GO) reduction can re-constitute the sp^2 graphite structure, but its tendency to get aggregated irreversibly alone is a crucial issue. For preventing the graphene aggregation problem and maintaining a large surface area, the functionalization employing nanoparticles (NPs), mainly inorganic NPs, is widely used by various research groups worldwide [9]. The hematite NPs, i.e., α-Fe_2O_3NPs, are n-type semiconductors having Eg =2.1 eV bandgap. It is the most stabilized form of iron oxide under normal conditions. Owing to its

***Corresponding author:** Gopinath Packirisamy (gopi@bt.iitr.ac.in); Rangadhar Pradhan (rangadhar@gmail.com)

Article #

IEEE Sensors Letters

low toxicity, economical, environmentally friendly, high theoretical capacitance, and natural abundance, it gives an interesting prospect to fabricate new adsorbents with different nanomaterials, for example, graphene-hematite nanocomposites that would exhibit better electrochemical performances.

The process of green synthesis is a technique that has contributed to the environment by reducing and eliminating toxic and hazardous waste [10]. In the present study, a green approach was adopted to prepare α-Fe_2O_3NPs_rGO nanocomposite using *Cinnamomum tamala* leaves, which served as a reducing and capping agent. Due to its stimulating, carminative, and hypoglycemic characteristics, it is regularly employed as a food garnish and is primarily used in the pharmaceutical industry.

Substrates, in addition to these nanomaterials, are crucial in developing the biosensing platform for determination of oral cancer. The screen-printed electrode (SPE) is recognized as a promising substrate due to its low background signal, ease of surface modification, and broad potential window. SPE is the most practical and economical approach for developing electrochemical biosensors and *in situ* evaluation because of their low cost, miniaturized size, linear output, low power, quick response, higher sensitivity, ability to operate at room temperature, and access with portable devices. Additionally, they offer the reference, auxiliary, and working electrodes in a single device [11].

Considering the above facts, this letter presents a facile, ultrasensitive, and affordable electrochemical immunosensing platform for CYFRA-21-1 biomarker determination using α-Fe_2O_3NPs_rGO nanocomposite on SPE. Further, this letter reports the green synthesized α-Fe_2O_3NPs_rGO nanocomposite based electrochemical SPE nanoplatform for CYFRA-21-1 determination for the first time. Besides, attempts have been made to characterize the immobilized anti-CYFRA-21-1 based electrode to analyze its electrochemical performance.

II. EXPERIMENTAL SECTION

A. Materials and chemicals

The antibody CYFRA-21-1 (anti-CYFRA-21-1) derived from monoclonal mouse, ferric nitrate nonahydrate ($Fe(NO_3)_3.9H_2O$), CYFRA-21-1 antigen (human), and graphite flakes were bought from Sigma Aldrich. Sodium monophosphate [NaH_2PO_4], potassium ferricyanide ($K_3[Fe(CN)_6]$), sodium diphosphate anhydrous [Na_2HPO_4], and potassium ferrocyanide ($K_4[Fe(CN)_6]$) has been purchased from Fisher Scientific. The commercialized gold-based SPEs were procured from Metrohm DropSens company, India.

B. Green synthesis of α-Fe_2O_3NPs and α-Fe_2O_3NPs@rGO composite

The *Cinnamomum tamala'* leaves extract was prepared by boiling the leaves in distilled water (DI) for 1h. The $(FeNO_3)_3{\cdot}9H_2O$ solution was selected as a precursor for α-Fe_2O_3NPs. To this solution, leaves extract was added at 80 ºC and, the obtained solution was centrifuged, as well as the pellet was collected after drying. Further, the product was calcinated for 5 h at 700 ºC in a muffle furnace to achieve α-Fe_2O_3NPs.

Next, the α-Fe_2O_3NPs_rGO was made by employing the ultra-sonication technique. For this, 30 mg GO (prepared utilizing the modified Hummer's approach) dispersed in 30 mL DI, followed by 3 h ultrasonication to exfoliate the GO sheets. This solution was then combined with an α-Fe_2O_3NPs solution (10 mg NPs/10 mL DI), ultrasonically processed (overnight), and lastly, rinsed and dried. In a similar way, GO was reduced to rGO through ultrasonication without α-Fe_2O_3NPs [12]. Later on, the composite was functionalized with (3-Aminopropyltriethoxysilane (APTES) for 24 h.

D. Development of the BSA/anti-CYFRA-21-1/APTES/α-Fe_2O_3NPs_rGO/SPE immunosensor

For the development of immunosensing platforms, direct immobilization of antibodies on the sensing zone of SPE was carried out. At first, the anti-CYFRA-21-1 stock solution has been made in PBS (pH 7.4) to obtain 50 µg/mL concentration. Later, antibody solution was combined with N-Hydroxy succinimide (NHS) as well as 1-Ethyl-3-(3-dimethylaminopropyl) carbodiimide (EDC) in the ratio of 2:1:1 and pre-incubated for 45 min at 4 ºC. This activated solution of anti-CYFRA-21-1 was drop-casted on the APTES/α-Fe_2O_3NPs_rGO/SPE electrodes (5 µL per electrode) uniformly and incubated for 6 h in a humid environment at 4 ºC for immobilizing through formation of covalent bond between the amine group of APTES functionalized nanocomposite and carboxyl group of anti-CYFRA-21-1. This step was followed by washing electrodes with PBS to remove unbounded antibodies and adding 2% BSA (2 µL) to impede the non-specific electrode area. The constructed BSA/anti-CYFRA-21-1/APTES/α-Fe_2O_3NPs_rGO/SPE immunosensing electrode was kept in the refrigerator for future experiment. Scheme 1 represents the nanocomposite synthesis and modification steps of the immunoplatform for detecting CYFRA-21-1 biomarker.

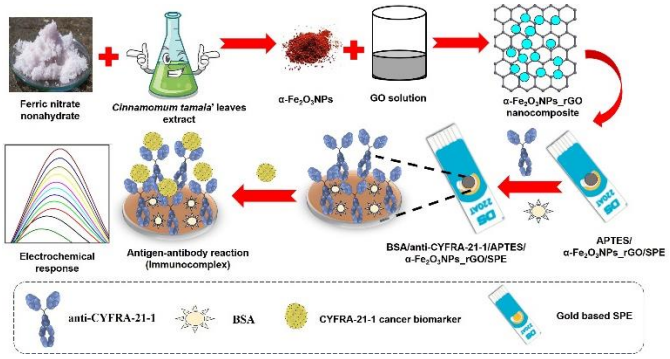

Scheme1. It represents the green synthesis of α-Fe_2O_3NPs_rGO nanocomposite as well as immunosensor fabrication towards CYFRA-21-1 cancer biomarker determination

III. Results and Discussions

A. XRD, and FTIR analysis

The XRD curve of α-Fe_2O_3NPs@rGO nanocomposite is depicted in Fig.1 (a). The various diffraction peaks were observed at 75.34º, 71.86º, 63.90º, 62.34º, 57.5º, 53.98º, 49.38º, 40.78º, 35.54º, 33.04º and 24.04º corresponding to (217), (208), (300), (214), (122), (116), (024), (113), (110), (104), and (012) planes, respectively of

IEEE Sensors Letters Article #

rhombohedral phase of Fe-O. These results are consistent with the data provided by the JCPDS No. 89–0599. In addition, the absence of peak at 2θ = 10º, (characteristic of GO) and presence of peak around 24º, further verifies the complete GO reduction to rGO in the nanocomposite.

The FTIR graph in the 4000-400 cm^{-1} range was done to demonstrate the chemical structures and functional groups present on APTES/α-Fe_2O_3NPs_rGO nanocomposite (Fig.1 (b). The graph depicts peaks at 1556, 1218, and 1017 cm^{-1} that are attributed to the C–C, epoxy C–O, as well as alkoxy C-O stretching vibrations of rGO aromatic skeletal, whereas peaks at 523 and 430 cm^{-1} corresponds to stretching vibrations of Fe-O bonds. In addition, the peak at 1410 cm^{-1} corresponds to the C-N stretching vibrations bond signifying the addition of amino group. This data thus, confirm the successful preparation of APTES/α-Fe_2O_3NPs_rGO nanocomposite.

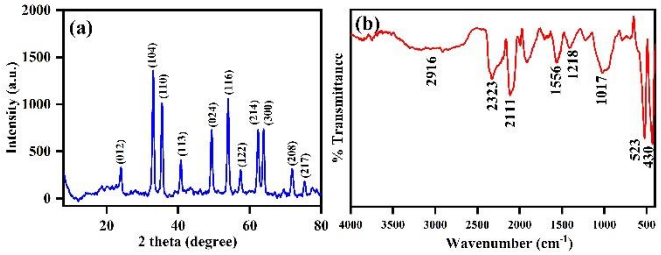

Fig.1 (a) XRD pattern of α-Fe_2O_3NPs_rGO composite and, (b) FTIR of APTES/α-Fe_2O_3NPs_rGO nanocomposite

B. Electrochemical analysis

The pH study was executed to observe the electrochemical performance of the constructed BSA/anti-CYFRA-21-1/APTES/α-Fe_2O_3NPs_rGO/ITO electrode employing the CV technique in PBS (0.2 M) buffer at numerous pH values i.e., 6.0 to 8.0 at 50 mV/s scan rate, having ferro-ferricyanide (5 mM) as a redox coupler in the potential widow from -0.8 to 0.8 V. The immunosensor electrode displays the highest peak current at pH 7.4 [Fig.2 (a)]. The reason behind it may be ascribed to the biological species involved (e.g., antibodies), which have large activity at neutral pH in their natural form. Further, in the basic or acidic media, antibodies' denaturation occurs owing to the existence of OH^-/H^+ ions. Hence, all the electrochemical experiments were executed in a PBS buffer (pH 7.4).

Further, the electrode modifications were executed using the cyclic voltammetry (CV) as well as differential pulse voltammetry (DPV) approaches. In Fig.2 (b), the CV of SPE (curve i), α-Fe_2O_3NPs/SPE (curve ii), rGO/SPE (curve iii), APTES/α-Fe_2O_3NPs_rGO/SPE (curve iv), anti-CYFRA-21-1/APTES/α-Fe_2O_3NPs_rGO/SPE (curve v), as well as BSA/anti-CYFRA-21-1/APTES/α-Fe2O3NPs_rGO/SPE (curve vi) electrodes, was measured respectively (Fig.2 (b)). The bare SPE oxidation peak current was reported at 36.43 µA (curve i). But in the case of α-Fe_2O_3NPs/SPE (curve ii), the current increases to 46.25 µA owing to the increase in surface area. The current further increases to 86.45 µA, when SPE was modified with APTES/α-Fe_2O_3NPs_rGO (curve iv) in comparison to rGO/SPE (78.37 µA, curve iii). This rise in anodic peak current might be due to the synergistic effect of both the nanomaterial's co-existence, i.e., of rGO as well as α-Fe_2O_3NPs that enhance the surface area, improved conductivity, and superior electrochemical properties [12]. However, the rise in peak current reached to 105.86 µA on immobilizing the anti-CYFRA-21-1. The presence of free NH_3^+ areas on the anti-CYFRA-21-1/APTES/α-Fe_2O_3NPs_rGO/SPE surface electrode may be the cause of elevation in peak current as it led to faster transfer of electrons between APTES/α-Fe_2O_3NPs_rGO/SPE electrode and anti-CYFRA-21-1 [13]. But, when the BSA proteins molecule is further drop casted at the surface of the immunoelectrode, they block non-specific areas of activity, preventing the transfer of electrons from the buffer to the electrode and lowering the BSA/anti-CYFRA-21-1/APTES/-Fe_2O_3NPs_rGO/SPE immunoelectrode' peak current to 73.95 µA. The similar trend of current concerning different electrodes were also supported by the DPV technique [Fig.2 (c)].

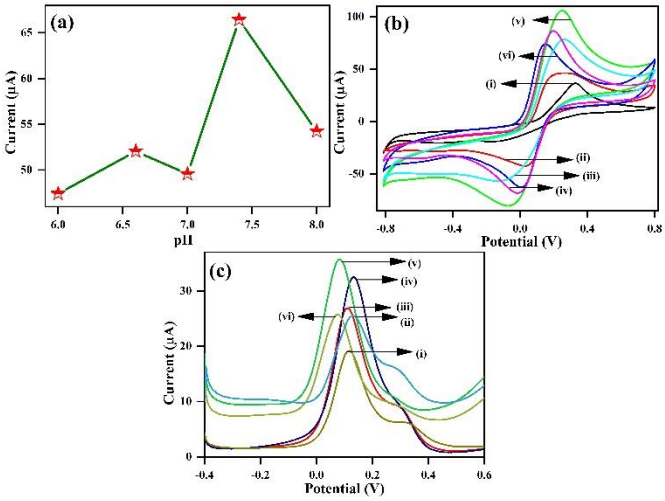

Fig.2 (a) It depicts the effect of various pH on biosensing electrode, Electrode studies using (b) CV and (c) DPV technique in PBS for different electrodes

The evaluation of the electrochemical performance of immunosensor was done using DPV method with respect to concentrations of CYFRA-21-1 cancer biomarker from 0.1 to 30 ng/mL (0.1, 0.5, 1.0, 3.0, 5.0, 10, 15, 20, 25 and 30 ng/mL) in PBS buffer having 5mM $[Fe(CN)]^{3-/4-}$ as presented by Fig.3 (a). The inset of this figure depicted an enlarged view of sensing towards CYFRA-21-1. It was observed that peak current showed enhancement with each addition of CYFRA-21-1 concentration, after which it gets saturated. This increasing trend in the electrochemical behavior of immunosensors arises due to immunocomplex formation (antigen-antibody) that occurred on the electrode surface between anti-CYFRA-21-1 as well as CYFRA-21-1 concentrations, thereby leading to the development of a faster electron transfer layer [14]. Moreover, Fig.3 (b) illustrates the linear correlation between the peak currents obtained by DPV as well as the CYFRA-21-1 concentrations. The regression coefficient (R^2) for this relationship is 0.960, as indicated by equation (1).

$$Ipa = [6.42(\mu A\ ng/mL) \times Conc.of\ CYFRA - 21 - 1\ (ng/mL) + 34.43\ \mu A], \quad R^2 = 0.960 \quad (1)$$

From the curve, the following electrochemical parameters were calculated, and the linearity range was achieved from 0.5-20 ng/mL,

Article #

IEEE Sensors Letters

the detection limit of 0.014 ng/mL, the limit of quantification (LOQ) of 0.048 ng/mL, and a very high sensitivity of 90.42 µA (log (ng/mL)$^{-1}$ cm^{-2}. The LOQ and detection limit was calculated using standard equations (2) and (3), respectively

$$LOQ = 10\sigma/Sensitivity \quad (2)$$

$$Detection\ limit = 3\sigma/\text{Sensitivity} \quad (3)$$

where σ depicts the BSA/anti-CYFRA-21-1/APTES/α-Fe_2O_3NPs_rGO/SPE immunoelectrode' standard deviation. Furthermore, immunoelectrode sensitivity was estimated utilizing equation (4):-

$$Sensitivity = Slope/area\ of\ immunoelectrode\ (0.071\ cm^2) \quad (4)$$

For checking the immunoplatform selectivity, different interfering agents existing in human saliva were made. For this purpose, inorganic ions of 100-times high concentration (e.g., NO_3^{-1}, Zn^{2+}, Na^+, $C1^-$, urea, K^+, Cu^{2+}, acetate, Fe^{2+}, ascorbic acid, SO_4^{2-} with respect to CYFRA-21-1 concentration were prepared. It can be seen from the bar graph [Fig.3 (c)] that negligible current change was recorded for the interfering elements as compared to immunoelectrode. In contrast, a decrement in peak current was observed for CYFRA-21-1 concentration (25 ng/mL), which indicates the specific interactions of immunoelectrode towards CYFRA-21-1 biomarker, indicating satisfactory relative standard deviation (%RSD) ranging from 1.37% to 8.39%.

Further, for the reproducibility evaluation of fabricated immunosensor, 6 different immunoelectrodes were developed at the same time using the DPV technique in PBS [bar diagram, Fig.3 (d)]. From the bar diagram, it could be observed that all immunoelectrodes' peak current was nearly the same, and the obtained %RSD value was calculated as 5.42%, suggesting high reproducibility of fabricated bioelectrodes.

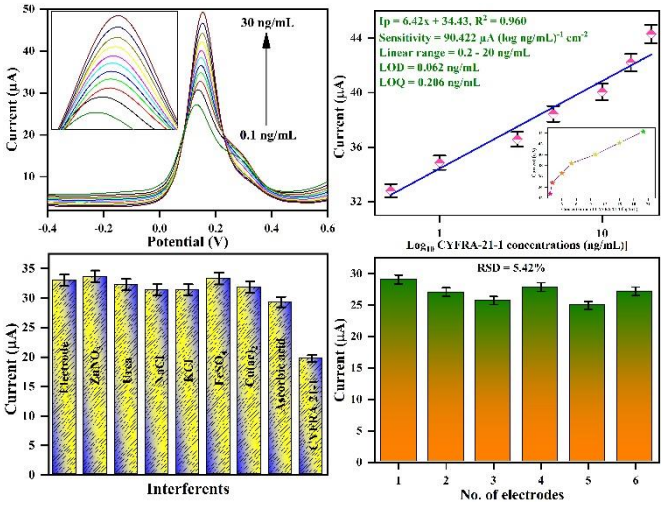

Fig.3 (a) Electrochemical response of immunosensor against CYFRA-21-1, (b) Linear plot of immunosensor current versus CYFRA-21-1 concentrations, (c) Interferents and, (d) Reproducibility studies of immunosensor

IV. CONCLUSION

In summary, we have demonstrated, for the first time, that the α-Fe_2O_3NPs_rGO nanocomposite prepared using the green method could be a robust material for electrochemical determination for CYFRA-21-1 cancer biomarker. Till now, no reports are there using green synthesized nanoplatform for CYFRA21-1 biomarker employing Fe_2O_3NPs_rGO nanocomposite on SPE. The BSA/anti-CYFRA-21-1/APTES/α-Fe_2O_3NPs_rGO/SPE immunosensor exhibits a broad linear detection range for CYFRA-21-1 having high sensitivity along with low detection limit and LOQ. The immunosensing platform also exhibits remarkable selectivity against CYFRA-21-1 with good reproducibility (%RSD =5.42%). Thus, the α-Fe_2O_3NPs@rGO nanocomposite would be a good potential candidate for the POC device development for real-time monitoring of oral cancer biomarkers.

ACKNOWLEDGMENT

Prof. GP appreciates the Indian Council of Medical Research (ICMR project No.5/13/34/GP/ICRC/2022/NCD-III) for funding. We also acknowledge the Institute Instrumentation Centre and Centre for Nanotechnology, IITR, Roorkee for providing the characterization facilities.

REFERENCES

[1] P. P. Dos Reis *et al.*, "Claudin 1 overexpression increases invasion and is associated with aggressive histological features in oral squamous cell carcinoma," *Cancer Interdiscip. Int. J. Am. Cancer Soc.*, vol. 113, no. 11, pp. 3169–3180, 2008.

[2] A. K. Markopoulos, E. Z. Michailidou, and G. Tzimagiorgis, "Salivary markers for oral cancer detection," *Open Dent. J.*, vol. 4, p. 172, 2010.

[3] R. Mehrotra and D. K. Gupta, "Exciting new advances in oral cancer diagnosis: avenues to early detection," *Head Neck Oncol.*, vol. 3, no. 1, pp. 1–9, 2011.

[4] E. B. Aydın, M. Aydın, and M. K. Sezgintürk, "Novel electrochemical biosensing platform based on conductive multilayer for sensitive and selective detection of CYFRA 21-1," *Sensors Actuators B Chem.*, vol. 378, p. 133208, 2023.

[5] D. Verma, A. K. Yadav, M. Das Mukherjee, and P. R. Solanki, "Fabrication of a sensitive electrochemical sensor platform using reduced graphene oxide-molybdenum trioxide nanocomposite for BPA detection: An endocrine disruptor," *J. Environ. Chem. Eng.*, vol. 9, no. 4, p. 105504, 2021.

[6] D. Verma, R. K. Sajwan, G. Lakshmi, A. Kumar, and P. R. Solanki, "A molecularly imprinted polymer based on a novel polyaniline–zinc sulfide nanocomposite for electrochemical detection of trimethylamine N-oxide," *Environ. Sci. Nano*, vol. 9, no. 10, pp. 3992–4006, 2022.

[7] A. K. Yadav, D. Verma, G. B. V. S. Lakshmi, S. Eremin, and P. R. Solanki, "Fabrication of label-free and ultrasensitive electrochemical immunosensor based on molybdenum disulfide nanoparticles modified disposable ITO: An analytical platform for antibiotic detection in food samples," *Food Chem.*, vol. 363, 2021, doi: 10.1016/j.foodchem.2021.130245.

[8] D. Verma, T. K. Dhiman, M. Das Mukherjee, and P. R. Solanki, "Electrophoretically Deposited Green Synthesized Silver Nanoparticles Anchored in Reduced Graphene Oxide Composite Based Electrochemical Sensor for Detection of Bisphenol A," *J. Electrochem. Soc.*, vol. 168, no. 9, 2021, doi: 10.1149/1945-7111/ac218a.

[9] M. Waqas *et al.*, "Fabrication of Non-enzymatic Electrochemical Glucose Sensor Based on Pd− Mn Alloy Nanoparticles Supported on Reduced Graphene Oxide," *Electroanalysis*, vol. 32, no. 6, pp. 1226–1236, 2020.

[10] D. Verma, D. Chauhan, M. Das Mukherjee, K. R. Ranjan, A. K. Yadav, and P. R. Solanki, "Development of MWCNT decorated with green synthesized AgNps-based electrochemical sensor for highly sensitive detection of BPA," *J. Appl. Electrochem.*, vol. 51, no. 3, 2021, doi: 10.1007/s10800-020-01511-3.

[11] J. P. Metters, R. O. Kadara, and C. E. Banks, "New directions in screen printed electroanalytical sensors: an overview of recent developments," *Analyst*, vol. 136, no. 6, pp. 1067–1076, 2011.

[12] D. Verma, K. R. Ranjan, M. Das Mukherjee, and P. R. Solanki, "Bioinspired synthesis of hematite nanoparticles-reduced graphene oxide composite for application in bisphenol a detection: A new in-sight," *Biosens. Bioelectron. X*, p. 100217, 2022.

[13] N. M. Fahrenkopf, P. Z. Rice, M. Bergkvist, N. A. Deskins, and N. C. Cady, "Immobilization mechanisms of deoxyribonucleic acid (DNA) to hafnium dioxide (HfO_2) surfaces for biosensing applications," *ACS Appl. Mater. Interfaces*, vol. 4, no. 10, pp. 5360–5368, 2012.

[14] S. Kumar, J. G. Sharma, S. Maji, and B. D. Malhotra, "Nanostructured zirconia decorated reduced graphene oxide based efficient biosensing platform for non-invasive oral cancer detection," *Biosens. Bioelectron.*, vol. 78, pp. 497–504, 2016.